Supporting information for: Lattice-Mismatched PbTe/ZnTe Heterostructure with High-Speed Midinfrared Photoresponses

Songsong Ma,[†,¶] Kai Li,[†,¶] Hanlun Xu,[†] Jiaqi Zhu,[†] Haiming Zhu,[‡] and Huizhen Wu[*,†]

†*Department of Physics, State Key Laboratory for Silicon Materials, Zhejiang University, Hangzhou 310027, China*

‡*Department of Chemistry, Zhejiang University, Hangzhou 310027, China*

¶*These authors contributed equally to this work.*

E-mail: hzwu@zju.edu.cn

1 Atomic force microscope images

The lattice constants of BaF_2, PbTe and ZnTe are 0.6200 nm, 0.6462 nm and 0.6101 nm respectively. The reason for choosing BaF_2 as substrates for PbTe epilayer is that their lattice constants and thermal expansion coefficients are close, so that the serious strain issue is avoided.[S1,S2] The atomic force microscope (AFM) image of PbTe epilayer demonstrates the very smooth surface with clear terrace structrues caused by spiral growth[S2] and root mean square roughness (RMS) as small as 0.374 nm, as shown in Fig. S1(a). Therefore, the PbTe epilayers are of high perfection. Because of the relatively large lattice mismatch between PbTe and ZnTe, the following ZnTe overlayers are not as smooth as PbTe layers. The surface RMS of ZnTe overlayers is 5.825 nm, as displayed in Fig. S1(b). However, the most crucial part for the PbTe/ZnTe heterostructure is the layers near the interface, and from the view of epatixy growth mechanism, the first few layers of ZnTe are supposed to adjust themself to match with the PbTe lattice. After stacking ZnTe for about several nanometers, the layers tend to recover to the ZnTe lattice constant due to strain accumulation, which leads to the relatively rough surface of ZnTe overlayer.

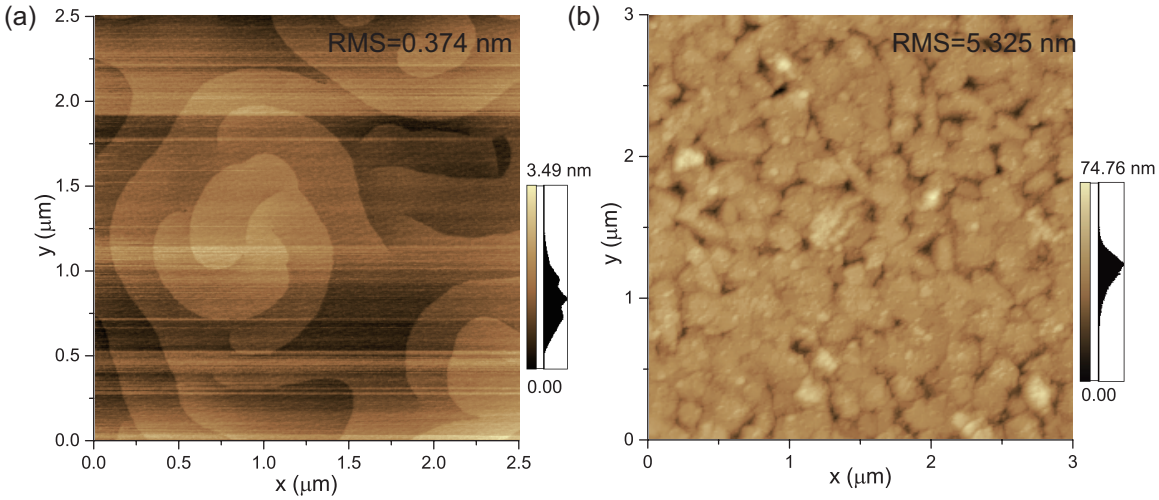

Figure S1: Surface morphology of (a) PbTe epilayer and (b) ZnTe overlayer characterized by AFM. The RMS roughness is denoted.

2 Forming Ohmic contact on PbTe/ZnTe heterostructure

To probe the transport properties of the conductive layer at the interface of PbTe/ZnTe heterostructure, the electrodes must be connected to the channel between PbTe and ZnTe, and the contact must be guaranteed to be Ohmic contact. We choose Cu to make electrodes via thermal evaporation, and with appropriate annealing process Cu can penetrate the thin ZnTe capping layer ($\sim$ 50 nm) to reach the conductive channel because Cu is a mobile element that is prone to diffuse, which has been well studied in the field of solar cell back contact.[S3] Furthermore, as presented in Fig. S2, the Cu-contacted PbTe/ZnTe heterostructures exhibits linear I-V characteristic for small current levels, which means no rectifying behaviour and indicates the formation of low-resistance Ohmic contact.

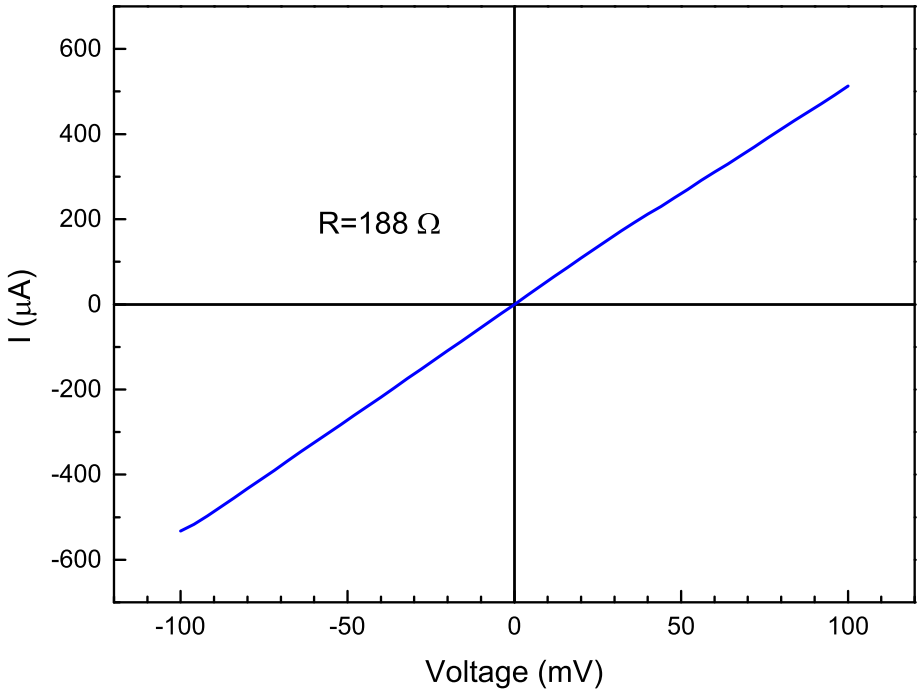

Figure S2: The I-V characteristic of PbTe/ZnTe heterostructure with Cu electrode forming Ohmic contact.

3 Bonding configuration of PbTe/ZnTe interfacial Te atoms

The crystal structures of PbTe and ZnTe are rock-salt and zincblende. In ZnTe, each Te atom has 4 nearest neighbour, which are Zn atoms. Therefore, as shown in Figure S3(a), each Te atom is bonded with 4 Zn atoms. Taking the four Zn atoms as vertices, we will obtain a regular tetrahedron. In the case of PbTe, each Te atom has 6 nearest neighbour, which are Pb atoms, so the Te atom is bonded with 6 Pb atoms, as shown in Figure S3(b). Taking the six Pb atoms as vertices, we will obtain a regular octahedron. However, in the PbTe/ZnTe(111) heterostructure, the interfacial Te atoms are shared by PbTe and ZnTe. Therefore, the interfacial Te atoms keep the tetrahedron bonding configuration with the ZnTe side, and keep the octahedron bonding configuration with the PbTe side. Consequently, each interfacial Te atom is bonded with 3 Zn atoms and 3 Pb atoms, as depicted in Figure S3(c). The model of PbTe/ZnTe(111) heterostructure is shown in Figure S3(d).

4 Bandoffset determined by XPS

The X-ray photoelectron spectroscopy (XPS) has been used to investigate the band offset at many heterostructures.[S4,S5] We present an experimental determination of the PbTe/ZnTe valence band offset (VBO) by XPS, and then the conduction band offset (CBO) is calculated from the obtained VBO value. Tab. S1 lists the values of core levels (CLs) and valence band maximum (VBM) by XPS spectrum fitting.

Table S1: The values of CL peaks and VBMs obtained from XPS spectra.

Sample	State	Binding Energy (eV)	Energy difference (eV)
PbTe	Pb $5d_{5/2}$	18.05	18.34
	VBM	-0.29	
ZnTe	Zn 3d	10.10	9.98
	VBM	0.12	
PbTe/ZnTe	Pb $5d_{5/2}$	18.09	-8.07
	Zn 3d	10.02	

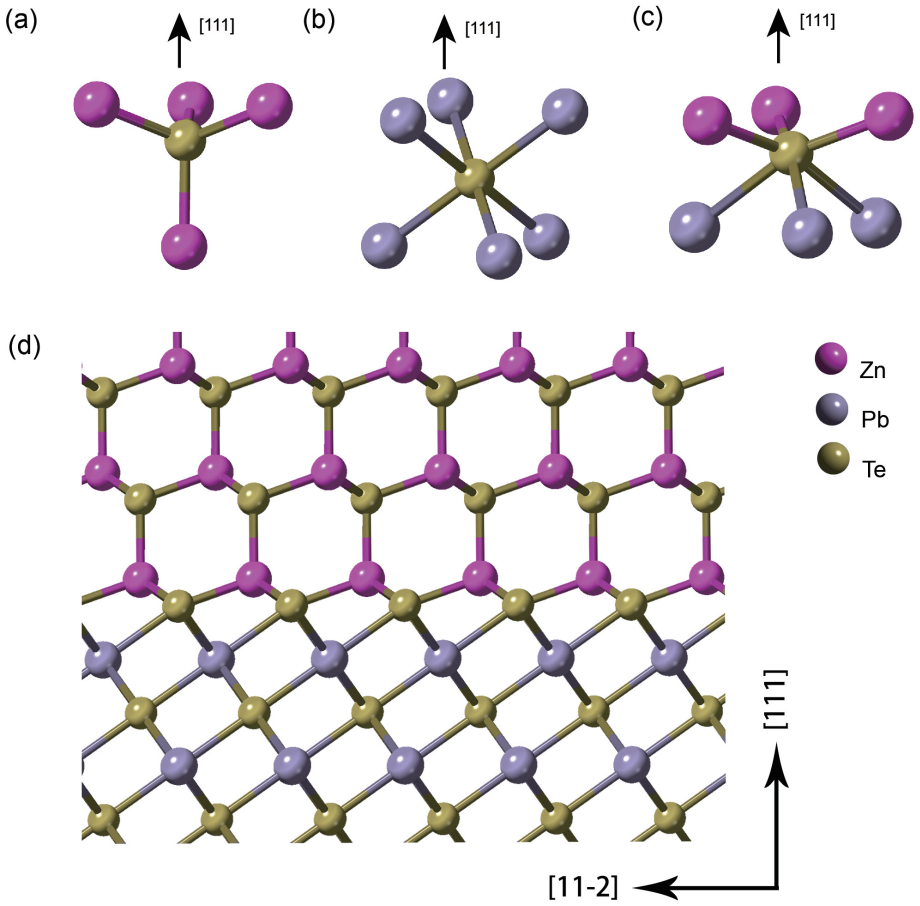

Figure S3: (a) Each Te atom in ZnTe is bonded with 4 Zn atoms forming a tetrahedron. (b) Each Te atom in PbTe is bonded with 6 Pb atoms forming a octahedron. (c) Each interfacial Te atom is bonded with 3 Pb atoms in PbTe side and 3 Zn atoms in ZnTe atoms.(d) The ball-stick model of the PbTe/ZnTe(111) heterostructure cross section.

5 Infrared photoresponse measurements

5.1 Responsivity spectrum

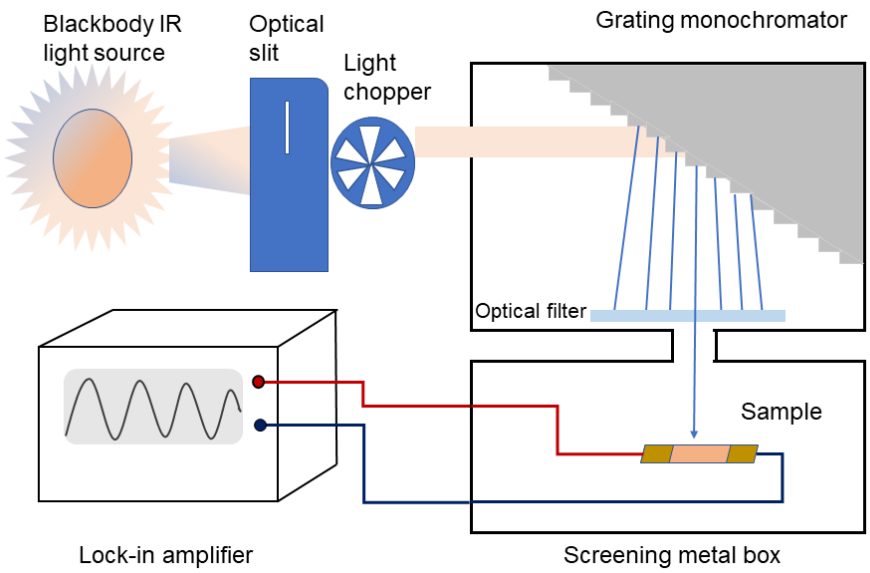

Figure S4: The IR photoresponse spectrum measurement system.

The photoresponse spectra are measured in a custom-built infrared (IR) photoresponse spectrum test system. The schematic diagram of the system is shown in Fig. S4. We adopt a blackbody IR light source in the measurement, the light of which is then modulated by a light chopper. Following the light chopper, a grating monochromator module covering a wavelength range from 1 μm to 10 μm is utilized to realize wavelength-resolved response spectrum measurement. After the monochromator, there are a series of optical filters corresponding to certain wavelength ranges, which are used to guarantee only the specific wavelength of light get through. The photodetector is mounted in a metal box screening the environmental light, and the incident illumination from the aforementioned monochromator module is shot on the detector. The photoresponse current/voltage signals could be collected through the wires connected to the electrodes. Because the incident light is modulated signal, we could use the standard lock-in amplifier to pick up the output signal. In our experiment, the incident light is chopped at a rate of 400 Hz.

Because the light intensity distribution is not uniform over the wavelength span, the as-measured photoresponse spectra cannot represent the standard responsivity of the detectors. To normalize the measured spectra, a standard commercial IR photodetector, whose standard responsivity spectrum data are known, is measured in our test system, and then the light intensity distribution can be obtained from the ratio of the measured and standard spectra of the commercial detector, enabling us to normalize the measured photoresponse spectra of our detectors.

5.2 Impulse photoresponse

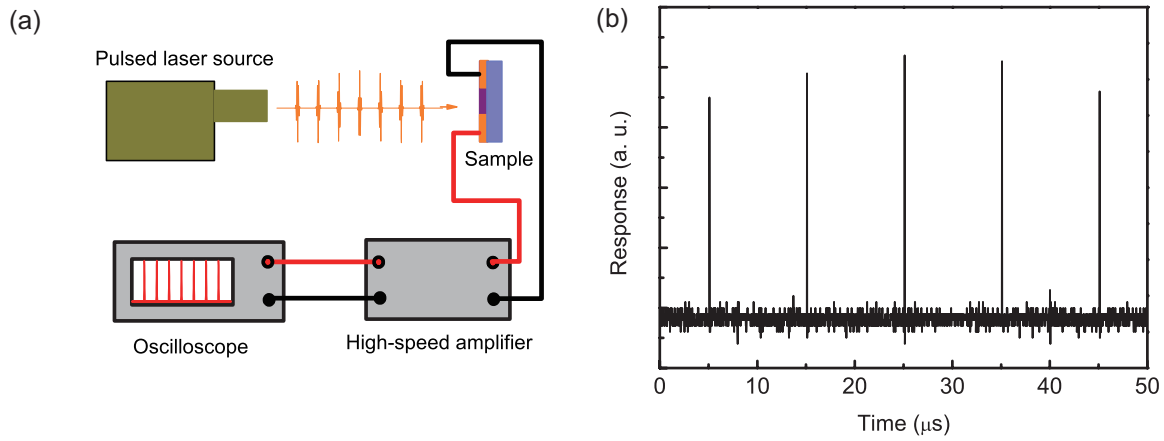

Figure S5: (a) The pulsed photoresponse measurement system. (b) Typical impulse photoresponse sequence under the illumination of a pulsed laser with single pulse duration on femtosecond timescale.

A pulsed laser source was used in the measurement of impulse photoresponses, with the duration of a single pulse on the femtosecond timescale and the repetition rate at 100 kHz. A high-speed amplifier with the bandwidth of 200 MHz and an oscilloscope were employed to single out the output signal. The schematic diagram of the measurement system is shown in Fig. S5(a) and a typical observed impulse sequence of photoresponse is displayed in Fig. S5(b).

Acknowledgement

The authors thank for the financial support from the National Natural Science Foundation of China (U1737109, 11933006) and Fundamental Research Funds for the Central Universities.

References

(S1) Holloway, H.; Logothetis, E. M.; Wilkes, E. Epitaxial Growth of Lead Tin Telluride. *Journal of Applied Physics* **1970**, *41*, 3543–3545.

(S2) Springholz, G.; Ueta, A. Y.; Frank, N.; Bauer, G. Spiral Growth and Threading Dislocations for Molecular Beam Epitaxy of PbTe on BaF_2 (111) Studied by Scanning Tunneling Microscopy. *Applied Physics Letters* **1996**, *69*, 2822–2824.

(S3) Li, J.; Diercks, D. R.; Ohno, T. R.; Warren, C. W.; Lonergan, M. C.; Beach, J. D.; Wolden, C. A. Controlled Activation of ZnTe:Cu Contacted CdTe Solar Cells Using Rapid Thermal Processing. *Solar Energy Materials and Solar Cells* **2015**, *133*, 208 – 215.

(S4) Zhang, R.; Zhang, P.; Kang, T.; Fan, H.; Liu, X.; Yang, S.; Wei, H.; Zhu, Q.; Wang, Z. Determination of the Valence Band Offset of Wurtzite InNZnO Heterojunction by X-ray Photoelectron Spectroscopy. *Applied Physics Letters* **2007**, *91*, 162104.

(S5) Si, J.; Jin, S.; Zhang, H.; Zhu, P.; Qiu, D.; Wu, H. Experimental Determination of Valence Band Offset at PbTe/CdTe(111) Heterojunction Interface by X-ray Photoelectron Spectroscopy. *Applied Physics Letters* **2008**, *93*, 202101.